Inorganica Chimica Acta 408 (2013) 172–180

Contents lists available at ScienceDirect

Inorganica Chimica Acta

journal homepage: www.elsevier.com/locate/ica

Ligand mediated structural diversity and role of different weak interactions in molecular self-assembly of a series of copper(II)–sodium(I) Schiff-base heterometallic complexes

Debabrata Biswas [a], Partha Pratim Chakrabarty [a], Sandip Saha [a,*], Atish Dipankar Jana [b,*], Dieter Schollmeyer [c], Santiago García-Granda [d]

[a] Department of Chemistry, AcharyaPrafulla Chandra College, New Barrackpur, Kolkata 700 131, India
[b] Department of Physics, Behala College, Parnasree, Kolkata 700 060, India
[c] Institut fur OrganischeChemie, Universit at Mainz, Duesbergweg 10-14, 55099 Mainz, Germany
[d] Departamento de QuímicaFísicayAnalítica, Universidad de Oviedo, C/JuliánClavería 8, 33006 Oviedo, Spain

ARTICLE INFO

Article history:
Received 15 June 2013
Received in revised form 3 September 2013
Accepted 4 September 2013
Available online 13 September 2013

Keywords:
Heterometallic
Schiff bases
Weak interactions
Supramolecular assembly
Tape motif
Self-organization

ABSTRACT

We report three new Cu–Na heterometallic complexes namely $[Cu(L1^{2-})Na(NO_3)(CH_3OH)]$ (**1**), $[Cu(L2^{2-})Na(NO_3)(CH_3OH)]$ (**2**) and $[Cu\ Na\ (L3^{3-})]_n$ (**3**) where the topology of the synthon is directly governed by the π–π interaction involving the Cu-Schiff base chelate rings. The crystal structure analysis also reveals how the systematic variation in the ligand framework influences the supramolecular assembly and the mutual cooperation of different π-forces and the hydrogen bonding forces in the supramolecular assembly. The π-forces are more important than the hydrogen bonding forces in such compounds is evident from the supramolecular assembly of compound **3**. Most interesting revelation of the studies are the presence of relatively uncommon π-forces such as chelate ring···chelate ring and metal–π interactions in the supramolecular architecture of the complexes. The analysis of the supramolecular assembly of the complexes **1**–**3** reveals that metal-chelate rings play prominent role in the organization of the molecular complexes and should seriously consider along with other π-stacking forces.

1. Introduction

Molecular self-assembly is the nature inspired methodology widely adopted in diverse areas of science and technology like supramolecular chemistry[1–7], crystal engineering [8–10], liquid crystal engineering [11–12], molecular electronics [13–15], biotechnology [16–17], host–guest chemistry[18–20], etc. Wide spread utilization of self-assembly has provided enough maturity to the field of crystal engineering which is the area where scientists aim the designed synthesis of crystalline materials where the molecular organization in the solid state can be reliably predicted from the knowledge of molecular tectons. In the endeavor of controlled organization of molecular building blocks generally various weak forces such as hydrogen bonding [21–29], π···π interaction [30–45], C–H···π interaction [46–50], metal-π interaction [47] have mostly been relied upon. Often particular hydrogen bonding synthon or a stable π-stacking motif has been employed to direct molecular units. In the design of molecular materials involving metal ions, additional consideration is the stereochemical information encoded in the metal ions which is revealed in the preferred coordination geometry of metal ions in the presence of a particular or a set of organic ligands. In this case ligand induced weak forces operate in a particular manner so that it can cooperate with coordinative forces but at times the weak forces can also compete with coordinative forces [51]. Prediction of the self-assembled structure is beset with the problem of accuracy due to the weak nature of directing forces. A slight perturbation in the physicochemical condition or a slight modification of the ligand framework generally leads to widely diverse self-assembled super structures. Designing a robust supramolecular motif is the key step in the reliable prediction of superstructure. Such robust recurring motifs are termed as "synthon" by G.R. Desiraju [52]. Usually the relatively strong hydrogen bonding forces are employed to design a robust supramolecular motifs, but other weak forces such as π-π and CH-π interactions are also suitable for designing such motifs. In the supramolecular assembly of the discrete metal–organic complexes the supramolecular assembly of discrete units are controlled by suitably designing the ligand. This involves tuning the coordination sites as well as organizing appropriate groups for hydrogen bonding or π-stacking on the ligand framework. Beyond the completely ligand centric π-stacking groups another stacking capable unit has emerged recently in square planar Cu, Ni and Pt complexes which

* Corresponding authors. Fax: +91 33 2537 8797.
E-mail addresses: sandipsaha2000@yahoo.com (S. Saha), atishdipankarjana@yahoo.in (A.D. Jana).

0020-1693/$ - see front matter © 2013 Elsevier B.V. All rights reserved.
http://dx.doi.org/10.1016/j.ica.2013.09.011

is the metal–ligand chelate ring [53–55]. It is intriguing that, even in the presence of ligand centric π-stacking moieties which are supposed to provide strong π-stacking sties, metal–ligand chelate rings in many cases exhibit π-stacking capability. The structures presented in the present paper are designed with an intention to explore the detailed nature of the competition between these two type of π-stacking sites. Recently we have shown that square planar Cu complexes can reliably be designed with Schiff bases resulting from the condensation of amines with hydroxylated aldehydes and saturating its remaining coordination sites by simultaneous use of auxiliary Na metal ions [56]. In the present paper we report a set of closely related Cu–Na hetero bimetallic complexes with suitably designed Schiff-base ligand bearing aromatic π-rings. The six coordination sites and two possible ligand centric π –interaction sites on Salicylaldimines with phenoxo groups in the 2 and 2′ positions render it suitable for coordinating various p- and d-block metal elements and also various alkali-metal ions [57–62] and subsequent intra complex supramolecular interaction. In the present study we have chosen Cu and Na along with a set of three closely related ligands H_2L1, H_2L2, H_3L3 and along with reported earlier [57] H_2L4 (Scheme 1) which differs from each other systematically.

We report three new Cu–Na heterometallic complexes namely $[Cu(L1^{2-})Na(NO_3)(CH_3OH)]$ (**1**), $[Cu(L2^{2-})Na(NO_3)(CH_3OH)]$ (**2**), and $[Cu\ Na\ (L3^{3-})]_n$ (**3**) where the topology of the supramolecular assembly is decisively influenced by the stacking interaction involving the Cu-Schiff base chelate rings.H_2L1, H_2L2 were synthesized in 1:2 condensation of 1,2-propane diamine and 1,3-propane diamine with 3-methoxy salicylaldehyde, respectively. The H_3L3 was produced in the same procedure by using 1, 3 diamino-2-propanol and 3-ethoxy salicylaldehyde. The analysis of the supramolecular assembly of the complexes **1**–**3** reveal that metal-chelate rings play prominent role in the organization of the molecular complexes and should seriously consider along with other π-stacking forces. We also compare our complexes with a similar set of three complexes reported by Bhowmick et al. [60] recently where they have highlighted the hydrogen bonding forces in the self-organization.

2. Experimental

2.1. Materials

All reagents and solvents were purchased from Sigma–Aldrich and were used as received. All other chemicals used were of analytical grade.

2.2. Physical measurements

IR spectra were recorded as KBr pellets within the range 4000–400 cm^{-1}on a Perkin-Elmer Spectrum 65 FTIR Spectrometer. Elemental analyses were carried out using a Heraeus CHN-O-Rapid elemental analyzer.

2.3. Syntheses

2.3.1. Synthesis of the ligands

The Schiff base ligands H_2L1, H_2L2 and H_2L4 were synthesized by refluxing1,2-propane diamine (0.074 ml, 1 mmol), 1,3-propane diamine (0.074 ml, 1 mmol) and ethylenediamine (0.06 ml, 1 mmol) with 3-methoxy salicylaldehyde (0.332 g, 2 mmol) in methanol (10 mL) for two hrs, respectively. The H_3L3 was produced in the same procedure by using 1,3 diamino-2-propanol (0.09 ml, 1 mmol) and 3-ethoxy salicylaldehyde (0.332 g, 2 mmol). The ligands were not isolated; instead the resulting yellow methanolic solutions were subsequently used for complex formation in every case.

2.3.2. Synthesis of complexes $[Cu(L1^{2-})Na(NO_3)(CH_3OH)]$ (**1**) and $[Cu(L2^{2-})Na\ (NO_3)\ (CH_3OH)]$ (**2**), $[Cu(L4^{2-})Na(NO_3)(CH_3OH)]$ (**4**)

A clear solution of $Cu(CH_3COOH)_2{\cdot}H_2O$ (0.199 g, 1 mmol) in methanol (10 ml) was added to a 10 mL methanolic solution of the H_2L1, and the mixed solution was stirred for 0.5 h. Aqueous solution of Sodium Nitrate(0.34 g, 4 mmol) dissolved in minimum volume of water was added drop wise to the resulting solution with constant stirring for 2 h. The reddish solution was filtered. On slow evaporation of the resulting reddish colored solution the dark red block shaped single crystal of the complex **1** was separated out in a few days. The crystals were filtered and washed with methanol and dried in air. The crystals of complex **2** and **4** were obtained in the same manner described above using yellow methanolic solution of H_2L2 and H_2L4 for complex **1**. Complex **4** was reported earlier by Cunningham et. al. [57] but our synthetic procedure is different and we have considered it for our weak interactions discussion section.

*Complex **1**:* Yield 65%. *Anal.* Cacl. for (complex **2**) $C_{20}H_{24}CuN_3NaO_8$: C, 46.06; H, 4.60; N, 8.06. Found: C, 46.07; H, 4.56; N, 8.1%. IR (KBr pellets, cm^{-1}): $\nu(CH_3OH)$ 3412, ν(C=N) 1638, $\nu(NO_3)$ 1384.

*Complex **2**:* Yield 70%. *Anal.* Cacl. for (complex **3**) $C_{20}H_{24}CuN_3NaO_8$: C, 46.06; H, 4.6; N, 8.06. Found: C, 46.1; H, 4.58; N, 8.04%. IR (KBr pellets, cm^{-1}): $\nu(CH_3OH)$ 3434, ν(C=N) 1628, $\nu(NO_3)$ 1384.

*Complex **4** (reported):* Yield 60%. *Anal.* Cacl. for (complex **1**) $C_{19}H_{22}CuN_3NaO_8$: C, 44.97; H, 4.33; N, 8.28. Found: C, 44.98 H, 4.3; N, 8.3%. IR (KBr pellets, cm^{-1}): $\nu(CH_3OH)$ 3435; ν(C=N) 1630; $\nu(NO_3)$ 1384.

2.3.3. Synthesis of complex **3**: $[Cu\ Na\ (L4^{3-})]_n$

A clear solution of $Cu(CH_3COOH)_2{\cdot}H_2O$ (0.199 g, 1 mmol) in methanol (10 ml) was added to a 5 ml methanolic solution of the H_3L3, and the mixed solution was stirred for 0.5 h. Aqueous solution of Sodium Nitrate dissolved in minimum amount of water (0.34 g, 4 mmol) was added dropwise to the resulting solution with

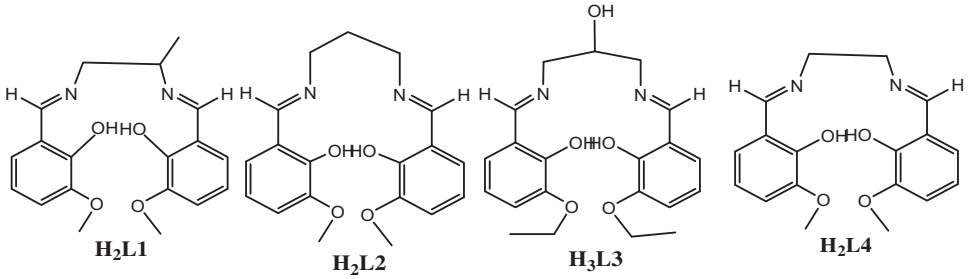

Scheme 1. Schematic presentation of the Schiff base ligands.

constant stirring for 2 h. The reddish solution was filtered. On slow evaporation of the resulting reddish colored solution the dark red block shaped single crystals of the complex **3** were separated out in a few days. The crystals were filtered and washed with methanol and dried in air.

*Complex **3**:* Yield 67%. *Anal.* Cacl. for (complex **3**) $C_{21}H_{23}CuN_2NaO_5$: C, 53.73; H, 4.9; N, 5.97. Found: C, 53.65; H: 4.86; N: 5.96%. IR (KBr pellets, cm^{-1}): ν(C=N) 1628, ν(Na–O) 3248, 3444, 3489.

3. Results and discussion

3.1. Synthesis

Compounds **1**–**2** were synthesized in a facile and identical manner. The Schiff base ligands produced by the 1:2 condensations of diamines with hydroxylated aldehydes in methanol solution were not isolated. Instead the yellow methanolicsolution produced were subsequently used for further preparation of the heterometallic complexes. When Na(I) is incorporated in the system the geometry of the Copper(II) ion is changed from square pyramidal to square planar. A slight modification in the ligand framework systems can play an important role for the designing of these types of heterometallic complexes which is evident from the single crystal structure analysis of Compounds **1** and **2**. Compounds **1** and **2** are Cu(II)–Na(I) dimeric compound as they possess similar kind of ligands set H_2L1, H_2L2 compared to compound **3** which is one dimensional Cu(II)–Na(I) polymer as it contains H_3L3 which is something different from the other ligands. Thus we can conclude that ligand mediated structural diversity can also be obtained.

3.2. X-ray crystal structure determinations

Single crystals of the title compounds (**1**–**3**) were harvested directly from the slow evaporation preparations and all cases suitable single crystals (i.e. those found by inspection to have well-defined morphology and that extinguished plane polarized light uniformly) were attached to the end of a MiTeGen mount using paratone oil. X-ray diffraction intensity data of the title compounds were collected at 173(2) K using a Bruker APEX-II CCD diffractometer equipped with graphite monochromated MoKα radiation (λ = 0.71073 Å). Data reduction was carried out using the program Bruker SAINT [63]. Because of very small values of the absorption coefficient, no absorption correction was applied. The structure of the title compounds were solved by direct method and refined by the full-matrix least-square technique on F^2 with anisotropic thermal parameters to describe the thermal motions of all non hydrogen atoms using the programs SHELXS97 and SHELXL97 [64,65] respectively. All the calculations were carried out using PLATON [66] and WinGX system Ver-1.64 [67]. All hydrogen atoms of the substituent groups were located from difference Fourier map and refined isotropically whereas all the hydrogen atoms attached to the ring carbons were placed at their geometrically idealized positions. The aromatic H-atoms were assigned isotropic temperature factors equal to 1.2 times the equivalent temperature factor of the parent atom whereas the displacement parameters for the hydrogen atoms were taken as $U_{iso}(H) = 1.5\ U_{eqv}$ (C) for $-CH_3$ groups. A summary of crystal data and relevant refinement parameters are given in Table 1. Selected bond distances and bond angles are given in Table 2 for compounds **1**–**3** and all the relevant H-bonding parameters are given in Table 3. All the relevant other weak interaction parameters for Cu···π, chelate-ring···chelate-ring, chelate-ring···π and π···π stacking interactions are given in Tables 4a–e.

3.3. Crystal structure description

3.3.1. Complex *1*

Single crystal X-ray structural analysis reveals that complex **1** is a discrete dinuclear system of Cu(II) and Na(I) simultaneously coordinated by the hexadentate ligand H_2L1 (Fig. 1). Cu1 possess square planar coordination geometry and Na1 has a distorted octahedral coordination with seven coordination bonds to O atoms. The dihedral angle between Cu1–L2 six member chelate

Table 1
Crystal data and structure refinement parameters for compounds (**1**)–(**3**).

	Crystal data (**1**)	Crystal data (**2**)	Crystal data (**3**)
Formula	$CuC_{20}H_{24}N_3NaO_8$	$CuC_{20}H_{24}N_3NaO_8$	$CuC_{21}H_{23}N_2NaO_5$
Formula weight	520.96	520.95	469.95
Crystal system	triclinic	triclinic	triclinic
Space group	$P\bar{1}$	$P\bar{1}$	$P\bar{1}$
a (Å)	7.1416(7)	7.2395(10)	8.3165(9)
b (Å)	11.6143(11)	11.3007(15)	10.5403(8)
c (Å)	14.1186(14)	13.4789(19)	13.2830(13)
α (°)	77.095(2)	96.090(3)	111.567(8)
β (°)	76.034(2)	99.796(3)	105.814(9)
γ (°)	77.487(2)	97.852(3)	95.450(7)
V (Å^3)	1091.22(18)	1067.0(3)	1016.78(19)
Z	2	2	2
D_{calc} (g/cm^3)	1.586	1.622	1.535
Mu(Mo Kα) (mm)	1.074	1.098	2.042
F(000)	538	538	486
Crystal size (mm)	.20 × .30 × .30	.10 × .27 × .27	.20 × .28 × .30
T (K)	173	173	293
Radiation (Å)	0.71073	0.71073	1.54184
θ Min–Max [°]	2.6, 26.2	1.8, 28.0	3.8, 70.6
Dataset	−8: 9; −15: 15; −18: 17	−9: 9; −12: 14; −17: 16	−9: 10; −12: 10; −16: 15
Tot., Uniq. Data, R_{int}	5285, 3976, 0.0328	12717, 5110, 0.025	6351, 3717, 0.044
Observed data [$I > 2.0\sigma(I)$]	3250	4460	2710
Nref, Npar	5285, 320	5110, 301	3717, 274
R, wR_2, S	0.0465, 0.1244, 1.025	0.0288, 0.0755, 1.03	0.0697, 0.2085, 0.99
Max. and Av. Shift/error	0.001, 0.00	0.00, 0.00	0.00, 0.00
Min. and Max. Resd. Dens. (e/Å^3)	−0.529, 1.314	−0.53, 0.81–0.33, 0.34	−0.72, 2.06

Table 2
Slecected bond distances and angles for compounds **1**–**3**.

Compound **1**		Compound **2**		Compound **3**	
Cu1–O19	1.884(2)	Cu1–O20	1.923(1)	C2–O1	1.445(5)
Cu1–O23	1.893(2)	Cu1–O23	1.938(1)	C3–O1	1.376(8)
Cu1–N8	1.97(1)	Cu1–N8	1.988(1)	C8–O3	1.309(6)
Cu1–N11	1.925(2)	Cu1–N12	1.998(2)	C9–N2	1.273(7)
Na2–O1L	2.386(3)	Na1–O1L	2.422(2)	C10–N2	1.466(6)
Na2–O2	2.511(3)	Na1–O1	2.626(2)	C11–O5	1.34(1)
Na2–O3	2.474(2)	Na1–O3	2.491(2)	C12–N1	1.471(8)
Na2–O19	2.337(2)	Na1–O21	2.419(1)	C13–N1	1.285(8)
Na2–O20	2.584(3)	Na1–O20	2.349(1)	C18–O2	1.365(6)
Na2–O23	2.368(3)	Na1–O23	2.375(2)	C19–O4	1.300(6)
Na2–O24	2.660(3)	Na1–O24	2.454(1)	N1– Cu1	1.958(4)
O1L–H1L	0.902(3)	O1L–H1L	0.962(1)	N2–Cu1	1.952(6)
O1L–C2L	1.417(4)	O1L–C2L	1.418(3)	O2–Na1	3.039(5)
N1–O2	1.257(3)	N1–O1	1.257(2)	O3 –Cu1	1.914(3)
N1–O3	1.244(4)	N1–O2	1.238(2)	O3–Na1	2.963(6)
N1–O4	1.244(4)	N1–O3	1.246(2)	O4–Cu1	1.901(4)
				O4–Na1	2.901(5)
				O5–Na1	2.771(9)
N8–Cu1–N11	84.4(3)	N8–Cu1–N12	97.05(6)	C12–N1–C13	118.1(5)
N8–Cu1–O19	171.5(3)	N8–Cu1–O20	91.94(6)	C12–N1–Cu1	117.0(4)
N8–Cu1–O23	95.3(3)	N8–Cu1–O23	171.89(6)	C13–N1–Cu1	124.1(4)
N11–Cu1–O19	94.7(1)	N12–Cu1–O20	170.35(6)	C9–N2–Cu1	124.2(4)
N11–Cu1–O23	179.6(1)	N12–Cu1–O23	91.05(6)	C10–N2–Cu1	115.7(4)
O19–Cu1–O23	85.56(9)	O20–Cu1–O23	79.95(5)	C18–O2–Na1	115.5(3)
O1L–Na2–O2	155.0(1)	O1–Na1–O3	49.62(5)	C21–O2–Na1	118.8(4)
O1L–Na2–O3	105.9(1)	O1–Na1–O20	106.89(5)	C8–O3–Cu1	123.2(3)
O1L–Na2–O19	105.76(9)	O1–Na1–O21	108.25(5)	C8–O3–Na1	129.2(3)
O1L–Na2–O20	87.53(9)	O1–Na1–O23	94.79(5)	Cu1–O3–Na1	103.8(2)
O1L–Na2–O23	98.93(9)	O1–Na1–O24	79.07(5)	C19–O4–Cu1	126.9(3)
O1L–Na2–O24	80.86(9)	O1–Na1–O1L	143.10(6)	C19–O4–Na1	119.8(3)
O2–Na2–O3	50.94(9)	O3–Na1–O20	136.71(6)	Cu1–O4–Na1	106.4(2)
O2–Na2–O19	98.54(9)	O3–Na1–O21	85.94(5)	C11–O5–Na1	111.6(5)
O2–Na2–O20	98.67(9)	O3–Na1–O23	139.56(6)	N1–Cu1–N2	89.8(2)
O2–Na2–O23	96.18(9)	O3–Na1–O24	86.29(5)	N1–Cu1–O3	159.6(2)
O2–Na2–O24	89.08(9)	O3–Na1–O1L	99.25(6)	N1–Cu1–O4	94.0(2)
O3–Na2–O19	133.6(1)	O20–Na1–O21	66.31(5)	N2–Cu1–O3	92.0(2)
O3–Na2–O20	85.92(9)	O20–Na1–O23	63.35(5)	N2–Cu1–O4	157.0(2)
O3–Na2–O23	138.8(1)	O20–Na1–O24	129.09(5)	O3–Cu1–O4	92.3(2)
O3–Na2–O24	90.34(9)	O20–Na1–O1L	109.95(5)	O2–Na1–O3	105.7(2)
O19–Na2–O20	62.64(8)	O21–Na1–O23	128.77(5)	O2–Na1–O4	51.9(1)
O19–Na2–O23	66.09(8)	O21–Na1–O24	161.34(5)	O2-Na1–O5	101.7(2)
O19–Na2–O24	127.55(9)	O21–Na1–O1L	84.88(5)	O3–Na1–O4	55.9(1)
O20–Na2–O23	128.09(9)	O23–Na1–O24	65.78(5)		
O20–Na2–O24	166.33(9)	O23–Na1–O1L	103.45(5)		
O23–Na2–O24	61.50(8)	O24–Na1–O1L	79.66(5)		

Table 3
Relevant hydrogen bonding parameters (Å, °).

	D–H···A	D–H	H···A	D···A	D–H···A	Symmetry
Compound **4** (reported)	O1L–H1L···O2	0.82	2.50	3.177(2)	140	$-1+x, y, z$
	O1L–H1L···O3	0.82	2.14	2.939(2)	163	$-1+x, y, z$
Compound **1**	O1L–H3···O2	0.90	2.01	2.874(2)	162	1655
Compound **2**	O1L–H1L···O2	0.96	2.02	2.930(2)	157	$-1+x, y, z$
	O1L–H1L···O3	0.96	2.46	3.280(2)	162	$-1+x, y, z$
	C7–H7···O1	0.95	2.56	3.476(2)	112	2665

ring planes (Cu1–N11–C12–C13–C14–O19) and (Cu1–N8–C7–C6–C1–O23) is 6.11(5)° which reflects that Cu1 posses square planar coordination geometry. Cu–N8, Cu–N11 bond distances are 1.97(1) Å and 1.925(2) Å while Cu1–O19 and Cu1–O23 bond distances are 1.884(2) and 1.893(2) Å, respectively. Na1 is coordinated by four O atoms donated by the ligand L2, two O atoms donated by a nitrate anion and a solvent methanol O (O1l) atom. Na2–O distances vary in the range 2.337(2)–2.660(3) Å.

Discrete dinuclear units are organized by cooperative hydrogen bonding and π···π forces in the (1 0 1) plane with a distinct 1D tape motif along the crystallographic *a*-axis (Fig. 2). Hydrogen bonding sites are provided by the trans axially coordinated nitrate anion and the methanol molecule to the Na(I) ion which act as self-complementary donor acceptor set between adjacent dinuclear units. The π forces arise from the aromatic as well as chelate rings involving the ligand L1 and the Cu(II) ion. Uncoordinated nitrate O atom act as acceptor for the methanol O–H donor group. The hydrogen bonded chains run along the crystallographic *a*-axis. Multiple π stacking interactions operate in unison with the hydrogen bonding forces. It is also notable that Cu···π interaction operates between Cu(II) ion and the aromatic ring .. along with this chelate-ring···chelate-ring and chelate-ring···π interactions form a dimeric subunit. These subunits are organized along the *a*-axis by chelate-ring···π and π···π interactions in cooperation with the

Table 4a
Geometrical parameters (Å, °) for the chelate-ring···π stacking interactions in compouns(**1**–**4**).

Rings *i*–*j*	Rc[a]	R1v[b]	α[d]	β[e]	Symmetry
*Compound **4** (reported)*					
R3···R4	3.8320(8)	−3.3915(5)	2.88(6)	27.61	−*x*, −*y*, −*z*
R3···R4	3.5015(8)	3.4906(8)	2.88(6)	18.65	1 − *x*, −*y*, −*z*
R2···R5 (Inter tape)	3.7699()	−3.3316(5)	3.28(6)	27.32	1 − *x*, −*y*, 1 − *z*
R2 = C1–C2–C3–C4–C5–C6; R3 = C1–C2–C3–C4–C5–C6; R5 = C1–C2–C3–C4–C5–C6					
*Compound **1***					
R3···R7	3.5753(19)	−3.2540(12)	5.01(14)	19.55	1 − *x*, −*y*, 1 − *z*
R3···R7	3.6734(19)	3.3440(12)	5.01(14)	20.83	2 − *x*, −*y*, 1 − *z*
R6···R4(Inter tape)	4.3710()	3.714	4.10	31.83	2 − *x*, −*y*, 1 − *z*
R3 = C1–C2–C3–C4–C5–C6; R4 = C1–C2–C3–C4–C5–C6; R6 = C1–C2–C3–C4–C5–C6; R7 = C1–C2–C3–C4–C5–C6					
*Compound **2***					
R1···R4	3.7303(10)	−3.4374(5)	2.21(7)	22.32	−*x*, 1 − *y*, −*z*
R1···R4	3.5667(10)	3.2544(5)	2.21(7)	22.42	1 − *x*, 1 − *y*, 1 − *z*
R1 = C1–C2–C3–C4–C5–C6; R4 = C1–C2–C3–C4–C5–C6					
*Compound **3***					
R2···R5	3.556(3)	3.219(2)	4.6(3)	20.70	1 − *x*, 1 − *y*, −*z*
R2 = C1–C2–C3–C4–C5–C6; R4 = C1–C2–C3–C4–C5–C6					

(Same references apply to Tables 4b–d).
[a] Centroid distance between ring i and ring j.
[b] Vertical distance from ring centroid i to ring j.
[d] Dihedral angle between the first ring mean plane and the second ring mean plane of the partner molecule.
[e] Angle between centroids of first ring and second ring mean planes.

Table 4b
Geometrical parameters (Å, °) for the chelate-ring···chelate-ring stacking interactions in compouns(**1**–**4**).

Rings *i*–*j*	Rc[a]	R1v[b]	α[d]	β[e]	Symmetry
*Compound **4** (reported)*					
R3···R3	3.7796(7)	3.7796(7)	0.0	28.98	1 − *x*, −*y*, −*z*
Compound **1**					
R3···R3	3.6249(16)	−3.2519(12)	0	26.22	1 − *x*, −*y*, 1 − *z*
*Compound **2***					
R1···R1	3.5215(9)	3.2727(5)	0	21.66	1 − *x*, 1 − *y*, 1 − *z*
*Compound **3***					
R2···R2	3.569(3)	3.246(2)	0	24.55	1 − *x*, 1 − *y*, −*z*

Table 4c
Geometrical parameters (Å, °) for the Cu···π interactions in compounds (**1**–**4**).

Rings *i*–*j*	Rc[a]	R1v[b]	α[d]	β[e]	Symmetry
*Compound **4** (reported)*					
R4···Cu1	3.746	3.196	31.42		1 − *x*, −*y*, −*z*
*Compound **1***					
R7···Cu1	3.765	3.372	26.43		1 − *x*, −*y*, 1 − *z*
*Compound **2***					
R4···Cu1	3.573	3.240	24.95		1 − *x*, 1 − *y*, −*z*
*Compound **3***					
R5···Cu1	3.656	3.247	27.36		1 − *x*, 1−*y*, −*z*

Table 4d
Geometrical parameters (Å, °) for the π···π interactions in compounds **1** and **2**.

Rings *i*–*j*	Rc[a]	R1v[b]	α[d]	β[e]	Symmetry
*Compound **1***					
R7···R7	3.617(2)	3.4293(14)	0	18.54	2 − *x*, −*y*, 1 − *z*
*Compound **2***					
R4···R4	3.6506(11)	−3.4626(7)	0	18.46	−*x*, 1 − *y*, −*z*

Table 4e
Geometrical parameters (Å, °) for the CH···π interactions in compounds **4** (reported) and **3**.

Rings *i*–*j*	Rc[a]	R1v[b]	α[d]	β[e]	Symmetry
*Compound **4** (reported)*					
C2L–H2LB···R5	2.96	23.38	138	68	1 + *x*, *y*, *z*
*Compound **3***					
C21–H21A···R2	2.67	23.38	150	55	−*x*, 1 − *y*, −*z*

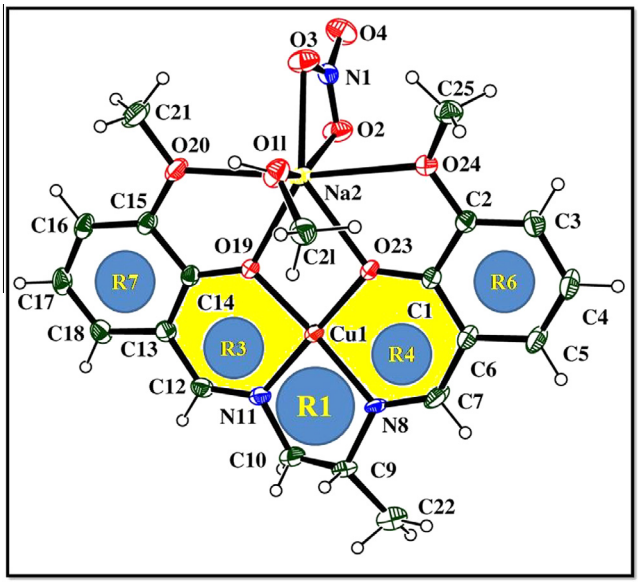

Fig. 1. ORTEP diagram (30% ellipsoidal probability) of **1**. (Rings R3, R4, R6 and R7 are involved in π-stacking interactions).

hydrogen bonding forces to produce the tape motif. Though these tapes are organized in the (1 0 1) plane in a similar fashion of **4** (reported complex), the inter tape chelate···π interaction is considerably weakened here (R6–R4 = 4.371 Å) compared to the chelate···π interaction in **4**. The packing of (1 0 1) layers are also

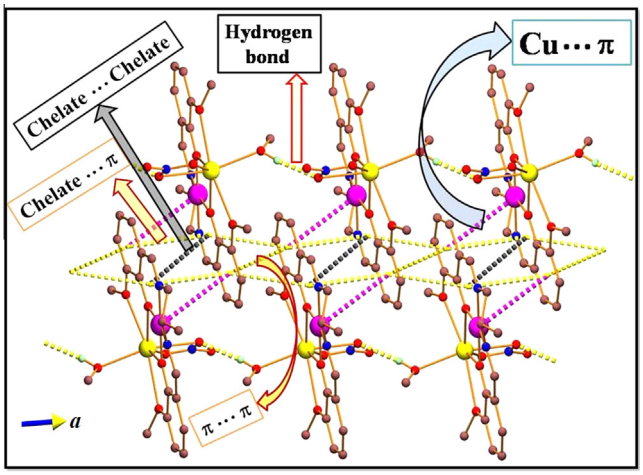

Fig. 2. The slef-assembled tape motif through Cu···π, chelate-ring···chelate-ring and chelate-ring···π interaction in **1**. Cu is shown in Magenta and Na in Yellow. (For interpretation of the references to colour in this figure legend, the reader is referred to the web version of this article.)

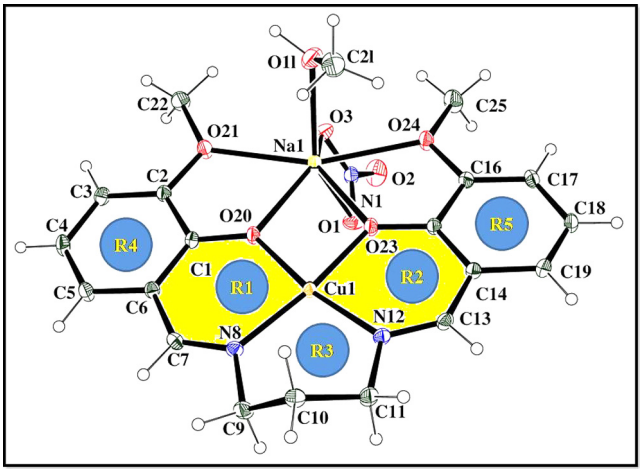

Fig. 3. ORTEP diagram (30% ellipsoidal probability) with atom numbering scheme of **2** (Rings R1, R2, R4 and R5 are involved in π-stacking interactions in the self-assembly of the depicted unit.)

of similar nature to **4** which are arranged side by side along the *b*-axis and the inter layer separation is governed by van der Waals forces (Fig. S1).

3.3.2. Complex **2**

Single crystal X-ray structural analysis reveals that complex **2** is a discrete dinuclear system of Cu(II) and Na(I) simultaneously coordinated by the hexadentate ligand H_2L2. While Cu1 posses square planar coordination geometry, Na1 is hepta coordinated with distorted octahedral coordination environment (Fig. 3). The dihedral angle between Cu1–L2 six member chelate ring planes (Cu1–N8–C7–C6–C1–O20) and (Cu1–N12–C13–C14–C15–O23) is 5.11(5)° which reflects that Cu1 posses square planar coordination geometry.

Cu1–N8, Cu1–N12 bond distances are 1.988(1) and 1.998(2) Å while Cu1–O20 and Cu1–O23 bond distances are 1.923(1) and 1.938(1) Å, respectively. Na1 is coordinated by four O atoms donated by the ligand L1, two O atoms donated by a nitrate anion

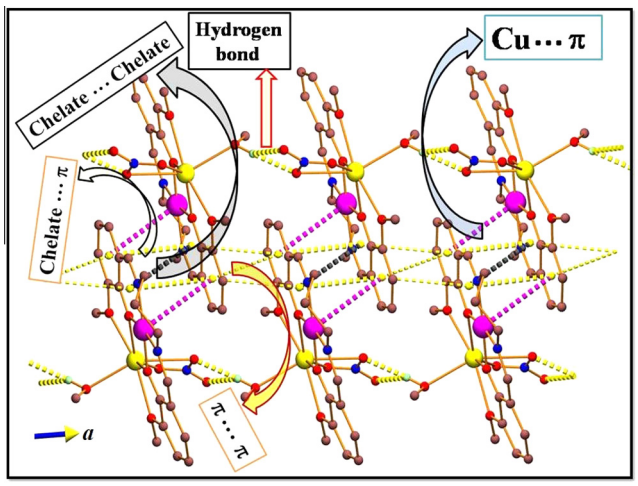

Fig. 4. The slef-assembled tape motif through Cu···π, chelate-ring···chelate-ring and chelate-ring···π interaction in **2**. Cu is shown in Magenta and Na in Yellow. (For interpretation of the references to colour in this figure legend, the reader is referred to the web version of this article.)

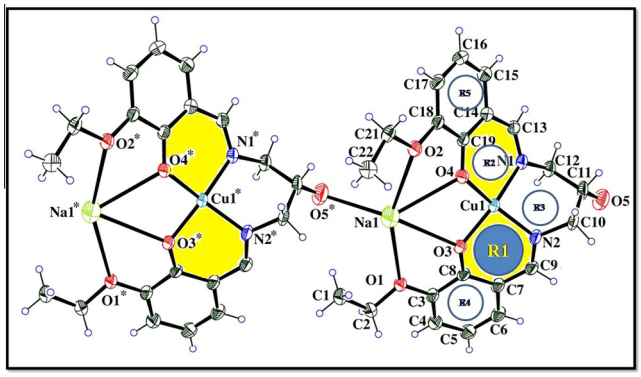

Fig. 5. ORTEP diagram (30% ellipsoidal probability) with atom numbering scheme of **3** (Rings R1, R2, R4 and R5 are involved in π-stacking interactions in the self-assembly of the depicted unit) [* = *x*, 1 + *y*, *z*].

and a solvent methanol O (O1l) atom. Na1–O distances vary in the range 2.349(1)–2.626(2) Å.

The nature of self-organization of dinuclear units in **2** is very close to that of **1**. Dinuclear units are arranged into 1D supramolecular tapes running along crystallographic *a*-axis (Fig. 4) by the similar set of Cu·π, chelate-ring·chetalte-ring, chelate-ring·π and π·π interactions. These are further organized side by side running parallel to each other in the *ac* plane (Fig. S2) by apparently weaker chelate·π interactions. At the next level of hierarchy these layers are stacked along the crystallographic *b*-axis like **1** and **2** by Vander-Waals forces.

3.3.3. Complex **3**

Single crystal X-ray structural analysis reveals that complex **3** is a 1D coordination chain of dinuclear units consisting of Cu(II) and Na(I) that are simultaneously coordinated by the hexadentate ligand H_3L3 (Fig. 5). Cu1–Na1 distance within a dinuclear unit is 3.893 Å. Cu1 possesses heavily distorted square planar coordination geometry. The angle between the two chelate ring planes Cu1–N1–C13–C14–C19–O4 and Cu1–O3–C8–C7–C9–N2 is 36.5(2)°. The Cu-N distances are slightly longer than the Cu–O distances. Whereas Cu1–O3 distance is 1.915(4) Å the Cu1–O4 distance is 1.902(4) Å. The Cu1–N1 and Cu1–N2 distances are

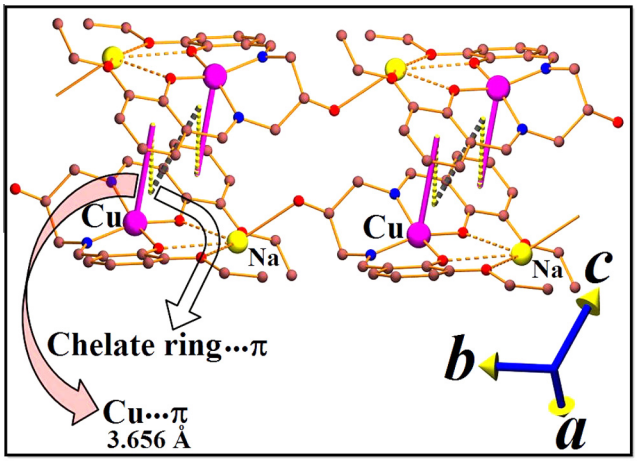

Fig. 6. Self-assembly of 1D coordination chains into 1D supramolecular tapes by Cu···π, chelate ring···π and chelate-ring···chelate-ring interaction in complex **3**.

1.958(5) and 1.951(5) Å respectively. The O3–Cu1–N2 angle is 92.03(18)° and the O4–Cu1–N1 angle is 93.99(18)°. Few other selective bond distances and angles are given in Table 2.

Na1 is unusually penta coordinated in the complex. It is coordinated by five O atoms present in the ligand. Four O atoms surround Na1 from one side in each unit and the translational symmetry related alcoholic oxygen atom (O5*, * = *x*, 1 + *y*, z) from an adjacent unit coordinate to Na1 from the opposite side. This coordination gives rise to one dimensional coordination polymeric chain of the dinuclear units. The coordination chains are aligned along the crystallographic *b*-axis. Among the four coordination from one side, Na1–O3 and Na1–O4 bond distances are relatively shorter (2.946(6) and 2.902(6) Å respectively) than the Na1–O1 and Na1–O2 distances (3.061(6) and 3.038(6) Å respectively). Na1–O5* distance is the shortest 2.770(8) Å among all the coordination bond lengths. The beauty of this structure lies in the deprotonation of the alkoxo hydroxyl group present in the middle position of the Schiff base ligand H_2L3. It is coordinated to the sodium ion after deprotonation and thus this unique one dimensional structure is obtained. It is to be noted that another Cu(II)–Na(I) dinuclear structure was reported recently with the similar kind of Schiff base [61] but no deprotonation occurred in that case.

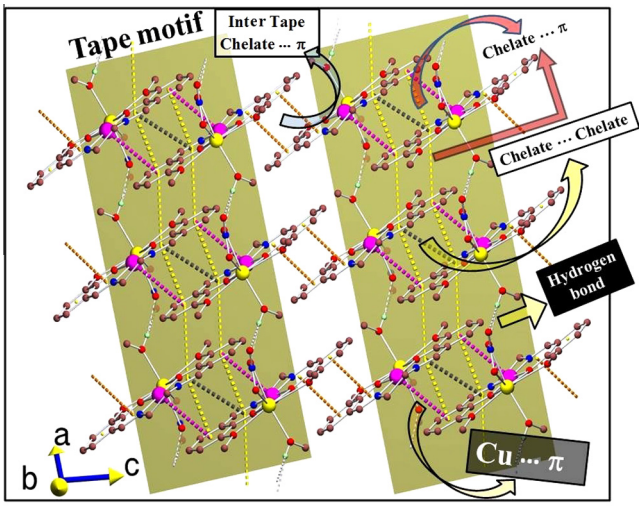

Fig. 7. The self-assembled tape motif through Cu···π, chelate-ring···chelate-ring and chelate-ring···π interaction and the 2D sheet the tapes joined by chelate-ring···π interaction in **4**. Cu is shown in Magenta and Na in Yellow. (For interpretation of the references to colour in this figure legend, the reader is referred to the web version of this article.)

1D coordination chains in complex **3** are further self-assembled into 1D tape motif in which two oppositely running self-complementary chains are recognized by each other through the concerted Cu···π, chelate ring···π and chelate-ring···chelate-ring interaction (Fig. 6).

3.3.4. Weak interactions present in reported complex **4**

Discrete dinuclear units are organized by weak force namely hydrogen bonding and π···π forces in the *ac* plane and forms a 2D supramolecular sheet (Fig. 7) with an embedded 1D tape motif running along the crystallographic *a*-axis. Whereas the hydrogen bonding sites are provided by coordinated NO_3 anion and the methanol molecule, the π forces involved are due to the aromatic phenyl rings on the H_2L4 ligand and the chelate rings formed due to coordination of ligand H_2L4 with Cu. The phenyl rings on H_2L4 are marked R4 and R5 whereas the six member chelate rings relevant for the stacking interactions are marked R2 and R3 in (Fig. S6). In the hydrogen bonding interaction the uncoordinated nitrate O atom act as acceptor for the methanol O–H donor group. The hydrogen bonded chains run along the crystallographic *a*-axis. Multiple π stacking interactions that operate in unison with the hydrogen bonding forces further stabilizes the hydrogen bonded chain and augments the dimensionality of the system into 2D through inter chain interaction. Besides these π stacking interactions, Cu···π interactions also come into effect. Detailed bonding paramets of the π-stacking interaction is given in Table 3. These supramolecular sheets are further organized side by side along the crystallographic *b*-axis (Fig. 8). Intra layer separation is equal to the length of the unit cell dimension along the *b*-axis and this is determined by the interlayer Van-der-Waals forces originating from the interactions between abundant $-CH_3$ groups present on adjacent stacking faces of successive layers.

3.3.5. Comparative discussions of the pattern of self-assembly

Three Cu(II) complexes reported here are closely related with identical coordination environment for Cu(II) and Na(I) except in **3** where a different coordination mode of Na(I) appeared. In each case Cu(II) assumes square planar coordination environment. In **1**–**2**, Na(I) assumes distorted octahedral coordination environment with the Schiff-bases binding in the equatorial plane and the trans axial sites occupied by a nitrate ion and a methanol molecule respectively. In **3** no methanol molecule or nitrate ion take part in the complexation, Na(I) is coordinated only by the O and N atoms on the Schiff-base which are five in number. The robust feature in the supramolecular self-assembly of complexes **1**, **2** and **4** is the appearance of a tape motif in each complex. The novel feature of this organization is the involvement of the Cu(II)-Schiff base chelate ring in the π-interaction between successive units. As has been described in the structural part, in each case chelate ring–chelate ring, chelate ring–π (aromatic), Cu–π (aromatic) interactions come into play in structuring the tape motif. Hydrogen bonding between Na centered nitrate ion and methanol molecule cooperate with these π forces. In **4**, these tapes are further united by chelate ring–π(aromatic) interactions into a two dimensional supramolecular sheet in the *ac* plane. In **1** and **2** this inter tape chelate ring–π(aromatic) interactions do not come into play. This is due to the presence of an additional $-CH_3$ group in H_2L1 and the additional central carbon atom in H_2L2 which rotates successive tapes in such a way that the inter tape chelate ring–π(aromatic) interactions in **1** and **2** become considerably weaker with long centroid to centroid distances (R3–R4 = 4.3710 Å in **2** and R2–R5 = 4.1102 Å in **3**). The presence of the central O atom (O5) in H_3L3 widely changes the mode of self-assembly in **3**. Here coordination of this O atom to an adjacent unit give rise to a 1D

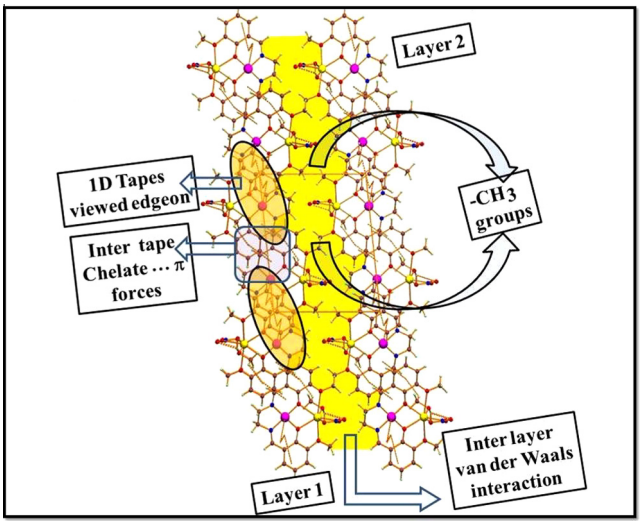

Fig. 8. Packing of successive (1 0 1) layers in **4** along *b*-axis.

coordination chain along the crystallographic *b*-axis (Fig. 5). Interestingly the inter-chain supramolecular association is again established through chelate ring–chelate ring, chelate ring–π (aromatic), Cu–π (aromatic) interactions giving rise to a tape motif along the *b*-axis. This motif is solely organized by π forces and no hydrogen bonding forces come into play.

Recently a similar set of three complexes were reported by Bhowmick et al. [60]where they have ignored the importance of π-forces in these complexes and have only stressed on the hydrogen bonding forces in the self-organization. When relooked and see that similar chelate ring–chelate ring, chelate ring–π (aromatic), Cu–π (aromatic) interactions are also present in these complexes (Figs. S3–S5 and Tables S1, S2a, S2b, S3a, S3b and S4). π interactions involving metal-chelate rings is a relatively new area in the self-assembly of molecular complexes and the present study shows that this interaction can play important role vis a vis other interactions and should be paid more attention in the design of molecular complexes. This study shows that Cu-ligand chelate ring possibly posses some kind of aromaticity.

4. Conclusion

Understanding the mutual role of multiple weak forces in the molecular self-assembly is emerging to be crucial in formulating the design principles in various areas of science and technology. Recently the metal–ligand chelate rings have been seen to take part in stacking interactions and in the present study we employ this interaction in the design of a set of three complexes. We see that instead of the ligand centric π–π interaction the chelate ring stacking interaction aided by Cu···π interaction governs the self-assembly of the molecular complexes. The solvent induced hydrogen bonding forces cooperate with these forces. With the design Schiff base ligands targeted square-planar Cu-Schiff base units can be achieved and the secondary alkali metal ion Na(I) provides the self-complementary hydrogen bonding sites through trans-axial coordination of the NO_3^- counter ion and CH_3OH solvent molecule. The primary Cu(II)-Schiff-base square plane motif is particularly amenable for stacking interactions involving the Cu-ligand chelate ring. Chelate ring of one unit interacts with both the phenyl ring and the chelate ring of adjacent unit. Chelate ring···chelate ring, chelate ring···π, Cu···π cooperate in the complexes. That the mutual interactions of these weak forces are quite subtle is revealed by the small but recognizable differences in the pattern of assembly due to small variations in the ligand frame work. The present study establishes that the recurrent tape motif in the self-assembly of the complexes is due to the π-stacking interaction involving the chelate ring of Cu and the Schiff-bases. That the hydrogen bonding forces merely cooperates with these π-forces is revealed in the self-assembly of compound **3** where hydrogen binding forces is absent but the tape motif recurs. In summary, in supramolecular design of Cu complexes the stacking interaction of Cu-ligand chelate ring should be paid more attention and can be utilized in the design of molecular materials.

Acknowledgements

Financial support from DST [Sanction no. SR/FT/CS-060/2009] and UGC [Sanction no.F.38-5/2009 (SR)], New Delhi to S. S. are gratefully acknowledged.

Appendix A. Supplementary material

CCDC 902506–902508 contains the supplementary crystallographic data for **1**–**3**. These data can be obtained free of charge from The Cambridge Crystallographic Data Centre via www.ccdc.cam.ac.uk/data_request/cif. Supplementary data associated with this article can be found, in the online version, at http://dx.doi.org/10.1016/j.ica.2013.09.011.

References

[1] B. Moulton, M.J. Zaworotko, Chem. Rev. 101 (2001) 1629.
[2] J.A. Thomas, J.L. Atwood, J.W. Steed (Eds.), Encyclopedia of Supramolecular Chemistry, CRC Press, Boca Raton, FL, 2004. p. 1248.
[3] D. Braga, L. Maini, M. Polito, L. Scaccianoce, G. Cojazzi, F. Grepioni, Coord. Chem. Rev. 225 (2001) 216.
[4] J.P. Sauvage (Ed.), Transition Metals in Supramolecular Chemistry: Perspectives in Supramolecular Chemistry, vol. 5, Wiley, London, 1999.
[5] G.R. Desiraju (Ed.), The Crystal as a Supramolecular Entity: Perspectives in Supramolecular Chemistry, vol. 2, Wiley, London, 1996.
[6] I.G. Dance, in: G.R. Desiraju (Ed.), The Crystals as a Supramolecular Entity, John Wiley, New York, 1996.
[7] A.D. Jana, S.C. Manna, G.M. Rosair, M.G.B. Drew, G. Mostafa, N.R. Chaudhuri, Cryst. Growth Des. 7 (2007) 1365.
[8] R.K. Seddon, M.J. Zaworotko, Crystal Engineering: The Design and Application of Functional Solids (NATO Science Series), 1999.
[9] G.R. Desiraju, Crystal Engineering: The Design of Organic Solids, Elsevier, Amsterdam, 1989.
[10] G.R. Desiraju, Angew. Chem., Int. Ed. 34 (1995) 2311.
[11] I.C. Khoo, Liquid Crystsl, Wiley-Interscience, A John Wiley and Sons, Inc. Publications, 2007.
[12] D.K. Yang, S.T. Wu, Fundamentals of Liquid Crystal Devices John Wiley & Sons, Ltd., 2006.
[13] C.D. Dimitrakopoulos, P.R.L. Malenfant, Adv. Mater. 14 (2002) 99.
[14] S.R. Forrest, Nature 428 (2004) 911.
[15] H. Meng, F. Sun, M.B. Goldfinger, F. Gao, D.J. Londono, W.J. Marshal, G.S. Blackman, K.D. Dobbs, E. Dalen, D.E. Keys, J. Am. Chem. Soc. 128 (2006) 9304.
[16] D.S. Godsell, Bionanotechnology lessons from nature, Wiley-Liss, A John Wiley & sons, Inc. publication, 2004.
[17] M.D. Cuyper, J.W.M. Bulte, Physics and Chemistry Basis of Biotechnology, Kulwar Academic Publishers 2002.
[18] T. Niu, A.J. Jacobson, Inorg. Chem. 38 (1999) 5346.
[19] K.K. Klausmeyer, T.B. Rauchfuss, S.R. Wilson, Angew. Chem., Int. Ed. 37 (1998) 1694.
[20] A.M.A. Ibrahim, Polyhedron 18 (1999) 2711.
[21] G.R. Desiraju, T. Steiner, The Weak Hydrogen Bond in Structural Chemistry and Biology, Oxford University Press, Oxford, 1999.
[22] G.A. Jeffrey, W. Saenger, Hydrogen Bonding in Biological Structures, Springer, Berlin, 1991.
[23] W.C. Hamilton, J.A. Ibers, Hydrogen Bonding in Solids, Benjamin, New York, 1968.
[24] S. Scheiner, Hydrogen Bonding: A Theoretical Perspective, Oxford University Press, Oxford, 1997.
[25] G.A. Jeffrey, An Introduction to Hydrogen Bonding, Oxford University Press, Oxford, 1997.
[26] T. Steiner, Angew. Chem., Int. Ed. 41 (2002) 48.
[27] Y. Zhang, Z. Yang, F. Yuan, H. Gu, P. Gao, B. Xu, J. Am. Chem. Soc. 126 (2004) 15028.
[28] S.I. Noro, T. Akutagawa, T. Nakamura, Cryst. Growth Des. 7 (2007) 1205.

[29] A.K. Ghosh, A.D. Jana, D. Ghoshal, G. Mostafa, N.R. Chaudhuri, Cryst. Growth Des. 6 (2006) 701.
[30] C.J. Janiak, Chem. Soc. Dalton Trans. (2000) 3885.
[31] O. Yamauchi, A. Odani, S. Hirota, Bull. Chem. Soc. Jpn. 74 (2001) 1525.
[32] M.J. Packer, M.P. Dauncey, C.A. Hunter, J. Mol. Biol. 295 (2000) 71.
[33] M.J. Packer, M.P. Dauncey, C.A. Hunter, J. Mol. Biol. 295 (2000) 85.
[34] K. Müller-Dethlefs, P. Hobza, Chem. Rev. 100 (2000) 143.
[35] R. Ghosh, A.D. Jana, S. Pal, G. Mostafa, H.K. Fun, B.K. Ghosh, Cryst. Eng. Commun. 9 (2007) 353.
[36] B.L. Schottel, H.T. Chifotides, M. Shatruk, A. Chouai, L.M. Perez, J. Bacsa, K.R. Dunbar, J. Am. Chem. Soc. 128 (2006) 5895.
[37] A.D. Jana, A.K. Ghosh, D. Ghoshal, G. Mostafa, N.R. Chaudhuri, Cryst. Eng. Commun. 9 (2007) 304.
[38] A.D. Jana, S.C. Manna, G.M. Rosair, M.G.B. Drew, G. Mostafa, N.R. Chaudhuri, Cryst. Growth Des. 7 (2007) 1365.
[39] P. Hobza, H.L. Selzle, E.W. Schlag, Chem. Rev. 94 (1994) 1767.
[40] K.S. Kim, P. Tarakeshwar, J.Y. Lee, Chem. Rev. 100 (2000) 4145.
[41] M.O. Sinnokrot, C.D. Sherrill, J. Phys. Chem. A 110 (2006) 10656.
[42] E.C. Lee, D. Kim, P. Jurecka, P. Tarakeshwar, P. Hobza, K.S. Kim, J. Phys. Chem. A 111 (2007) 3446.
[43] M. Pitonak, P. Neogrady, J. Rezac, P. Jurecka, M. Urban, P. Hobza, J. Chem. Theory Comput. 4 (2008) 1829.
[44] N.J. Singh, S.K. Min, D.Y. Kim, K.S. Kim, J. Chem. Theory Comput. 5 (2009) 515.
[45] E.A. Mayer, R.K. Castellano, F. Diederich, Angew. Chem., Int. Ed. 42 (2003) 1210.
[46] M. Nishio, M. Hirota, Y. Umezawa, The C–H···π Interaction: Evidence, Nature and Consequences, Wiley–VCH, New York, 1998.
[47] M. Nishio, Cryst. Eng. Commun. 6 (2004) 130.
[48] M.d.C. Fernandez-Alonso, F.J. Canada, J. Jimenez-Barbero, G. Cuevas, J. Am. Chem. Soc. 127 (2005) 7379.
[49] D. Braga, S.L. Giaffreda, F. Grepioni, L. Maini, M. Polito, Coord. Chem. Rev. 250 (2006) 1267.
[50] H.J. Schneider, Angew. Chem., Int. Ed. 48 (2009) 3924.
[51] J.J. Jiang, Y.R. Liu, R. Yang, M. Pan, R. Cao, C.Y. Su, Cryst. Eng. Commun. 10 (2008) 1147.
[52] G.R. Desiraju, Angew. Chem., Int. Ed. Engl. 34 (1995) 2311.
[53] A. Michaelides, S. Skoulika, V. Kiritsis, C. Raptopoulou, A. Terzis, J. Chem. Res. (S) (1997) 204.
[54] MilosK. Milčić, Vesna B. Medaković, Snežana D. Zarić, Inorg. Chimi. Acta 359 (2006) 4427.
[55] R.T. Edward, Chem. Commun. 47 (2011) 6623.
[56] P.P. Chakrabarty, D. Biswas, S. García-Granda, A.D. Jana, S. Saha, Polyhedron 35 (2012) 108.
[57] D. Cunningham, P. McArdle, M. Mitchell, N.N. Chonchubhair, M.O. Gara, Inorg. Chem. 39 (2000) 1639.
[58] Y. Sui, D.P. Li, C.H. Li, X.H. Zhou, T. Wu, X.Z. You, Inorg. Chem. 49 (2010) 1286.
[59] M. Das, S. Chatterjee, S. Chattopadhyay, Inorg. Chem. Commun. 14 (2011) 1337.
[60] P. Bhowmik, S. Jana, P.P. Jana, K. Harms, S. Chattopadhyay, Inorg. Chim. Acta 390 (2012) 53.
[61] M. Dolai, M. Mistri, A. Panja, M. Ali, Inorg. Chim. Acta 399 (2013) 95.
[62] S. Biswas, S. Naiya, M.G.B. Drew, C. Estarellas, A. Frontera, A. Ghosh, Inorg. Chim. Acta 266 (2011) 219.
[63] SMART, and SADABS, Bruker AXS Inc. Madison, Wisconsin, USA.
[64] G.M. Sheldrick, SHELXS-97 and SHELXL-97, University of Göttingen, Germany, 1997.
[65] G.M. Sheldrick, Acta Crystallogr., Sect. A 64 (2008) 112.
[66] A.L. Spek, J. Appl. Crystallogr. 36 (2003) 7.
[67] L.J. Farrugia, J. Appl. Crystallogr. 32 (1999) 837.